附件1-16 论文16 本项目成员关伟鹏、陈邦栋、黄谋潇为论文作者

Optical Engineering

OpticalEngineering.SPIEDigitalLibrary.org

High-precision indoor three-dimensional positioning system based on visible light communication using modified artificial fish swarm algorithm

Shangsheng Wen
Xiaoge Cai
Weipeng Guan
Jiajia Jiang
Bangdong Chen
Mouxiao Huang

SPIE.

Shangsheng Wen, Xiaoge Cai, Weipeng Guan, Jiajia Jiang, Bangdong Chen, Mouxiao Huang, "High-precision indoor three-dimensional positioning system based on visible light communication using modified artificial fish swarm algorithm," *Opt. Eng.* **57**(10), 106102 (2018), doi: 10.1117/1.OE.57.10.106102.

Downloaded From: https://www.spiedigitallibrary.org/journals/Optical-Engineering on 1/23/2019
Terms of Use: https://www.spiedigitallibrary.org/terms-of-use

High-precision indoor three-dimensional positioning system based on visible light communication using modified artificial fish swarm algorithm

Shangsheng Wen,[a] Xiaoge Cai,[b] Weipeng Guan,[b,*] Jiajia Jiang,[c] Bangdong Chen,[c] and Mouxiao Huang[b]
[a]South China University of Technology, School of Materials Science and Engineering, Guangzhou, China
[b]South China University of Technology, School of Automation Science and Engineering, Guangzhou, China
[c]South China University of Technology, School of Electronic and Information Engineering, Guangzhou, China

Abstract. Indoor visible light positioning has become a research hotspot owing to its high accuracy, low cost, and easy implementation. However, many existing indoor positioning systems based on visible light communication (VLC) can only achieve two-dimensional (2-D) positioning and those focusing on three-dimensional (3-D) positioning usually contain various sensors or use complex algorithms. Consequently, a high-precision indoor 3-D positioning system based on VLC using modified artificial fish swarm algorithm is proposed, avoiding the problems mentioned above. To simplify the solution procedure of searching for 3-D coordinates, the 3-D positioning problem is transformed into a global optimization problem with the corresponding fitness function designed according to Lambertian radiation pattern. The simulation executed on 1350 points shows an average 3-D positioning error of 4.05 mm in an indoor space of 4 m × 4 m × 6 m, and 90% positioning errors are below 5.95 mm. Moreover, when tracking a moving target in the positioning space, the average error is 3.57 mm and the maximum error is 7.25 mm. All in all, the system proposed in this paper stands a good chance of widespread application for its excellent performance in indoor 3-D positioning. © *2018 Society of Photo-Optical Instrumentation Engineers (SPIE)* [DOI: 10.1117/1.OE.57.10.106102]

Keywords: visible light communication; positioning accuracy; indoor three-dimensional positioning; modified artificial fish swarm algorithm; global optimization.

Paper 180781 received Jun. 6, 2018; accepted for publication Sep. 7, 2018; published online Oct. 5, 2018.

1 Introduction

With the emergence of various large structures, such as shopping malls, transit interchanges, hospitals, and so on, the indoor activity places become more and more complicated. Meanwhile, demands on indoor positioning and navigation for multifarious location-based services present a significant growing trend. As radio signals from satellites will be greatly weakened by the obstruction of tall buildings, GPS is far from a practical system in indoor environments for its low positioning accuracy.[1] Hence, it has attracted worldwide interest and investigation to develop new systems for indoor positioning. To date, based on various technologies including wireless local area network (WLAN),[2] bluetooth,[3] radio-frequency identification (RFID),[4] ultrawide band (UWB),[5] and infrared (IR),[6] numerous new-type indoor positioning systems (IPSs) have been proposed. However, WLAN is usually used together with fingerprinting identification, for which a great deal of complex work needs to be completed previously to establish a database. Moreover, such positioning systems are likely to suffer a long response time if the database is large. Both bluetooth- and WLAN-based IPSs are difficult to obtain a high positioning accuracy due to the multipath effect. Although RFID-, UWB-, and IR-based IPSs are able to achieve high positioning accuracy in centimeters, they are costly for implementation and extensive deployment on account of the requirements for additional infrastructure and new hardware components. Furthermore, there are some other deficiencies of these systems, such as electromagnetic interference, narrow tracking range, and low confidentiality.

As a new solution to indoor positioning, visible light positioning (VLP) is generally considered as a promising scheme for its obvious advantages of high positioning accuracy, no electromagnetic interference, fewer extra modules, and high confidentiality.[7] In the IPSs based on visible light communication (VLC), light-emitting diodes (LEDs) not only provide illumination for indoor environment but also play indispensable roles in communication and positioning as signal transmitters. In the other words, VLC-based IPSs perfectly make an integration of lighting and communication, contributing to a lower cost.[8] Generally, IPSs based on VLC are divided into two formats according to the differences of receivers: photodiode-based (PD-based) and image sensor-based (IS-based).[9] IS-based positioning systems require potent support of complex image processing techniques, which set a great demand on the perfect performance of systems.[10] Therefore, PD-based positioning systems are more practical compared to IS-based systems with the advantages of simplicity, reliability, and low cost. In PD-based VLP systems, a PD is able to estimate the distance between itself and the signal sources by detecting the light properties, such as received signal strength (RSS), angle of arrival (AOA),[11] time of arrival,[12] and time difference of arrival.[13]

With the positioning cost, complexity, and accuracy taken into consideration, RSS-based technique is the preference among all the methods mentioned above. Hence, many researchers have made intensive studies on it. However,

*Address all correspondence to: Weipeng Guan, E-mail: gwpscut@163.com; augwpscut@mail.scut.edu.cn

0091-3286/2018/$25.00 © 2018 SPIE

Downloaded From: https://www.spiedigitallibrary.org/journals/Optical-Engineering on 1/23/2019
Terms of Use: https://www.spiedigitallibrary.org/terms-of-use

most of these previous works only focused on two-dimensional positioning (2-D positioning) or suffered from plenty of limitations in realizing three-dimensional positioning (3-D positioning). For example, Yang et al.[14] used a single transmitter and multiple receivers to realize 2-D positioning based on RSS and the relative position of receivers, making the average positioning error as low as 0.65 cm. In Ref. 15, Jung defined received signal strength ratio (RSSR) between the received signals and introduced the distance ratio factors to obtain the function of RSSR with three equations included, so the location of terminal could be calculated by solving the three equations. However, this method had only achieved 2-D positioning. To realize 3-D positioning, in Ref. 16, Vellambi used an optical receiver and an accelerometer to, respectively, measure the RSS and orientation at the same time. In such a positioning system, on one hand, adding an extra accelerometer increased the cost. On the other hand, the synchronicity problem needed to be solved thereby making the positioning process more complex. Hou et al.[17] put forward a hybrid algorithm based on the link application of RSS and AOA, by which 3-D positioning with an average error of 10.2 cm was actualized. But the hybrid algorithm inevitably increased the difficulties in calculation. Lim[18] proposed a maximum likelihood approach for RSS-based indoor 3-D VLP. As Newton–Raphson iterative method was used in the estimation process, the performance of this method depended heavily on the initial predictions. That is to say, it might suffer a long response time and a large error or even fail to converge if starting with an awful guess. According to the analyses above, all these systems failed to provide a satisfactory performance in indoor 3-D positioning.

In recent years, some researchers have tried to apply bio-inspired algorithms to positioning. For example, Li et al.[19] proposed a new positioning method in nonline-of-sight environment, which use genetic algorithm (GA) to obtain a relatively accurate initial value and least square (LS) algorithm to update the position estimation. Lai et al.[20] applied particle swarm optimization to 3-D positioning based on laser range finder. Inspired by these works, a high-precision indoor 3-D positioning system based on VLC using a modified artificial fish swam algorithm (MAFSA) is proposed to solve the problems mentioned in the last paragraph. AFSA is a powerful population-based bionic evolutionary algorithm for global optimization problems.[21,22] As the RSS-based 3-D positioning problem can be transformed into a global optimization problem, AFSA is supposed to have an outstanding performance in indoor 3-D positioning by searching for the optimal 3-D coordinates of the positioning terminal. However, as the research progresses, it is ascertained that AFSA usually suffers a long convergence time due to the inhibition of the crowding factor on the clustering of artificial fish. Therefore, a more efficient and simpler MAFSA with the crowding factor discarded is proposed to take the place of AFSA in indoor 3-D positioning based on VLC. Furthermore, the results of a series of simulations prove the superiority of MAFSA and the prominent performance of the proposed system.

The rest of the paper is organized as follows: in Sec. 2, the model of IPS based on VLC is described concretely, and a detailed introduction of MAFSA is provided. Section 3 shows the analyses of the simulation results to verify the remarkable performance of the proposed indoor 3-D positioning system. Finally, the conclusion of this paper is given in Sec. 4.

2 System Principle and Positioning Algorithm

2.1 *Indoor Optical Wireless Channel*

As shown in Fig. 1, the proposed indoor VLP system mainly consists of two parts: (1) four LED bulbs acting as transmitters and (2) a mobile terminal acting as a receiver. In the system, the four LEDs are installed at the ceiling, emitting the visible light to provide illumination for indoor environment. It is worth mentioning that the visible light from LEDs is modulated using code division multiple access (CDMA) technology, which is confirmed to make a difference in reducing the intercell interference in our previous work.[23–25] As a result, the overlapping signals from different LEDs can be distinguished. Meanwhile, the unique ID information representing the 3-D coordinates of each LED can be transmitted through the modulated optical signals.

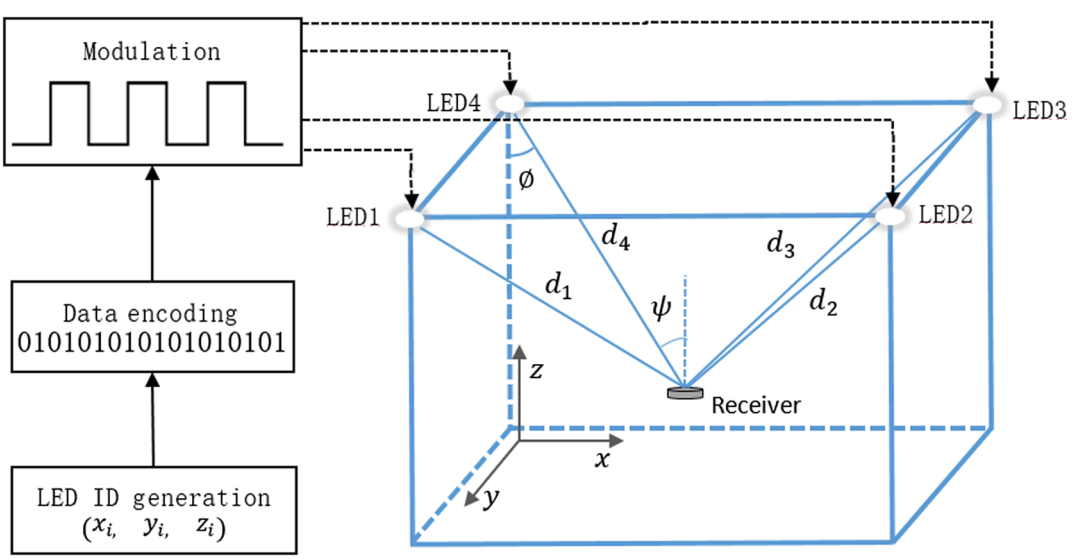

Fig. 1 The model of indoor 3-D positioning system based on VLC.

Downloaded From: https://www.spiedigitallibrary.org/journals/Optical-Engineering on 1/23/2019
Terms of Use: https://www.spiedigitallibrary.org/terms-of-use

Correspondingly, a PD installed on the mobile terminal recognizes the signals from different LEDs and detects the RSS separately.

Although there is nonline-of-sight (NLOS) channel in optical wireless communication apart from line-of-sight (LOS) channel, only the LOS channel is taken into consideration in this paper for the purpose of simplifying the positioning model. On the assumption that the luminous intensity of LEDs follows Lambertian radiation pattern,[10] the optical channel gain of the LOS channel $H_{\mathrm{LOS}}(0)$ can be expressed as

$$H_{\mathrm{LOS}}(0)=\begin{cases}\frac{A(m+1)}{2\pi d^2}T_s(\psi)G(\psi)\cos^m(\phi)\cos(\psi) & 0\le\psi\le\psi_c\\ 0 & \psi\ge\psi_c\end{cases}, \tag{1}$$

where A is the effective area of the PD. m is the Lambertian parameter defined as $m=\frac{-\ln 2}{\ln(\cos\phi_{1/2})}$, where $\phi_{1/2}$ is the half-power angle of a LED. d is the distance between the receiver and a LED. ϕ is the emission angle, ψ is the incidence angle, and ψ_c is the field-of-view (FOV) of the receiver, respectively. $T_s(\psi)$ is the gain of an optical filter, and $G(\psi)$ is the gain of an optical concentrator.

In essence, $H_{\mathrm{LOS}}(0)$ is defined as $H_{\mathrm{LOS}}(0)=\frac{P_{\mathrm{LOS}}}{P_t}$, where P_t is the emitting optical power of a LED. P_{LOS} is the incident optical power from LOS channel and the corresponding electrical power P_r can be given by $P_r=R(\lambda P_{\mathrm{LOS}})^2$, where R is the equivalent impedance of the receiver and λ is the response of the PD. According to Eq. (1), in a VLC-based IPS without any optical filter and concentrator, P_r can be further expressed as[26]

$$P_r=\frac{C}{d^4}\cos^{2m}(\phi)\cos^2(\psi), \tag{2}$$

where C is a constant determined by the system, and it can be calculated as

$$C=\frac{R\lambda^2A^2(m+1)^2P_t^2}{4\pi^2}. \tag{3}$$

In a practical system, the total incidence optical power P_{total} contains the incident optical power from LOS channel P_{LOS} and NLOS channel P_{NLOS} as well as the incident optical power from other light sources in the background $P_{\mathrm{background}}$. As only LOS channel is used for positioning in this paper, both P_{NLOS} and $P_{\mathrm{background}}$ are considered as noise power. Hence, the total noise variance can be given as

$$\sigma^2_{\mathrm{noise}}=\sigma^2_{\mathrm{shot}}+\sigma^2_{\mathrm{thermal}}+R(\lambda P_{\mathrm{NLOS}})^2, \tag{4}$$

where σ^2_{shot} is the shot noise variance depending on P_{total}, and $\sigma^2_{\mathrm{thermal}}$ is the thermal noise variance depending on the receiver's parameters. σ^2_{shot}, $\sigma^2_{\mathrm{thermal}}$, and P_{NLOS} are described detailedly in Ref. 27. The signal-to-noise ratio (SNR) of the proposed system can be defined as

$$\mathrm{SNR}=10\log_{10}\left(\frac{P_r}{\sigma^2_{\mathrm{noise}}}\right). \tag{5}$$

2.2 *Conversion from Positioning to Optimization Problem*

In the proposed VLP system, a 3-D spatial coordinate system is set up, in which the 3-D coordinates of each LED are labeled as (x_i,y_i,z_i), $(i=1,2,3,4)$, and the coordinates of the receiver are assumed as (x_r,y_r,z_r).

The key to RSS-based positioning is to estimate the distance between the receiver and transmitter by detecting and analyzing the RSS. In an indoor PD-based VLP system, what can be detected directly is the corresponding electrical power P_r that is transformed from the incident optical power from LOS channel P_{LOS} by a PD. Through the analyses of indoor optical wireless channel in Sec. 2.1, the relationship between d and P_r has been established. On the assumption that the receiver is parallel to the ceiling, the incidence angle ψ is equal to the emission angle ϕ and both of them can be calculated by $\psi=\phi=\cos^{-1}(\frac{z_i-z_r}{d_i})$, where d_i $(i=1,2,3,4)$ is the distance between the i'th LED and receiver. According to Eq. (2), d_i can be estimated as

$$d_i=\left[\frac{C(z_i-z_r)^{2m+2}}{P_{ri}}\right]^{\frac{1}{2m+6}}. \tag{6}$$

Theoretically, the distance between an arbitrary point (x,y,z) and the i'th LED should be

$$d_i'=\sqrt{(x-x_i)^2+(y-y_i)^2+(z-z_i)^2}. \tag{7}$$

Here, the difference between d_i' and d_i is defined as

$$\Delta d_i=|d_i'-d_i|. \tag{8}$$

As for the receiver, Δd_i should also be zero ideally. In other words, if a point (x,y,z) in the positioning space meets the condition that $\Delta d_i=0$ holds for $i=1,2,3,4$, it can be judged as the location of the receiver. In this case, an equation-set with four equations included can be used to solve the three unknowns (x,y,z). However, as the equation of Δd_i is quite complex, the equations set is too difficult to solve with analytical methods. Moreover, it is uncertain whether there is a set of solutions to the equations set or not due to the measurement and estimating errors.

To avoid the adverse situation mentioned above and simplify the solution procedure, the problem of indoor 3-D positioning is transformed into a global optimization problem, for which, the objective function is set up as

$$\Delta d=\sum_i^4\Delta d_i. \tag{9}$$

Then, to estimate the location of the receiver is essentially to search out a point that minimizes Δd in the positioning space.

2.3 *Modified Artificial Fish Swam Algorithm for Indoor Localization*

AFSA is a global optimization algorithm inspired by the foraging behaviors of shoal. In water, the basic behavior of a fish is to search for regions with more food either by vision or sense. Generally, the place with more fish is the place with

Downloaded From: https://www.spiedigitallibrary.org/journals/Optical-Engineering on 1/23/2019
Terms of Use: https://www.spiedigitallibrary.org/terms-of-use

more nutriments, as well as the solution space of the optimization problem. Imitating the true fish in nature, each artificial fish is able to accept the stimulus information from the external environment and act accordingly. Although the external environment is mainly determined by the solution space of the optimization problem and the statuses of other individuals.[22]

For the optimization problem transformed from indoor 3-D positioning, the target variables are 3-D coordinates, so the state of artificial fish is formulated as

$$X_j = (x_j, y_j, z_j), \qquad (j = 1,2, \cdots n), \tag{10}$$

where n is the population quantity of the artificial fish swarm. The fitness function of an artificial fish is given as Fitness $= f(X_j) = \Delta d$ and lesser value of fitness function means higher consistency of food because the optimization problem in this paper is a minimizing problem. According to the fitness, each individual searches for better states in the iteration procedure via four behaviors including preying, swarming, following, and moving described as follows.

2.3.1 *Preying operator*

Naturally, the fish will move toward regions with higher consistency of food. With the current state of an artificial fish assumed to be X_j, the individual randomly selects a state X_v within its visual range

$$X_v = X_j + \text{Visual} \times \text{Rand}(). \tag{11}$$

If $f(X_v) < f(X_j)$, it moves a step toward X_v and reaches a next state X_{next}:

$$X_{\text{next}} = X_j + \frac{X_v - X_j}{\|X_v - X_j\|} \times \text{Step} \times \text{Rand}(), \tag{12}$$

where $\|\cdot\|$ is the Euclidean distance between the two states. On the contrary, if $f(X_v) \geq f(X_j)$, it reselects a state X_v for another try. If its failure time meets the try-number set as an upper limit of attempt time, it will move a step randomly as Eq. (16).

2.3.2 *Swarming operator*

The fish usually moves in crowds to avoid danger. For an individual, nf is the number of its fellows within the visual distance. If $nf \neq 0$, the center position of the small group is defined as

$$X_c = \sum_{j}^{nf} \frac{X_j}{nf}. \tag{13}$$

If $nf \times f(X_c) < \delta \times f(X_j)$ and $f(X_c) < f(X_j)$, where δ is the crowding factor of the artificial fish swarm, it moves a step toward X_c and reaches a next state X_{next}:

$$X_{\text{next}} = X_j + \frac{X_c - X_j}{\|X_c - X_j\|} \times \text{Step} \times \text{Rand}(). \tag{14}$$

And if not so, it executes the preying behavior.

2.3.3 *Following operator*

When a fish succeeds in discovering a region with more food, the neighboring fish will tail it for food. For a fish, X_b is the best individual within the visual range and the number of individuals around the best fish is nf. If $nf \times f(X_b) < \delta \times f(X_j)$ and $f(X_b) < f(X_j)$, the fish will move a step toward the best individual and reach a next state X_{next}:

$$X_{\text{next}} = X_j + \frac{X_b - X_j}{\|X_b - X_j\|} \times \text{Step} \times \text{Rand}(). \tag{15}$$

If not so, it executes the preying behavior.

2.3.4 *Moving operator*

The fish moves randomly when it fails in preying or fails to reach a better state after evaluating the three behaviors above.

$$X_{\text{next}} = X_j + \text{Step} * \text{Rand}(). \tag{16}$$

Considering that the crowding factor δ may result in a slow convergence rate and low estimating accuracy for its inhibition on the clustering of artificial fish, it is ignored in MAFSA, which is the main difference between MAFSA and AFSA. The concrete flow of MAFSA is shown in Fig. 2 and the detailed description is given as follows:

Step 1: Set initial value. With a series of relevant parameters set, including the population quantity n, the visual distance visual, the step value step, the upper limit of attempt time try – number, the ideal fitness $\text{Fit}_{\text{ideal}}$, and the max iteration Iter_{max}, all the artificial fish are distributed in the positioning space randomly with states $X_j = (x_j, y_j, z_j)$, $(j = 1,2, \cdots n)$.

Step 2: Calculate fitness and initialize the bulletin. First, calculate the fitness of each artificial fish $f(X_j)$. Then, find out the best individual by comparing the calculated fitness and record its state on the bulletin.

Step 3: Update the state of each fish. Each artificial fish executes the three behaviors including preying, swarming, and following to get three different X_{next}. Then, an evaluation on the three behaviors is made to find out the best next state X_{bnext} by comparing the fitness of the three different X_{next}. If $f(X_{\text{bnext}}) < f(X_j)$, substitute X_j with X_{bnext} as the new state. If $f(X_{\text{bnext}}) \geq f(X_j)$, the artificial fish moves a step randomly to reach a new state.

Step 4: Update the bulletin. After updating the states of all fish, calculate their fitness and find out the best individual. Compared with the state recorded on the bulletin, if the fitness of the best individual is better, update the bulletin with the state of the best individual, otherwise, keep the bulletin the same.

Step 5: Iterate cyclically. Completing the update of bulletin, judge whether the termination condition has been met, if so output the state recorded on the bulletin as the positioning result, if not, repeat steps 2 to 4.

Downloaded From: https://www.spiedigitallibrary.org/journals/Optical-Engineering on 1/23/2019
Terms of Use: https://www.spiedigitallibrary.org/terms-of-use

3 Simulation Results and Analysis

3.1 *Three-Dimensional Indoor Location Simulation Model*

Executing simulations in software is a convenient way to evaluate the performance of MAFSA and investigate the proposed indoor 3-D positioning system based on VLC. As shown in Fig. 1, in a room with a size of 4 m × 4 m × 6 m, four LEDs are installed at the four corners of the ceiling and transmit their unique signals modulated with CDMA technology. The terminal to be positioned recognizes these signals and measures the strengths of them separately. The main parameters of the model are shown in Table 1. It is worth noting that the ideal fitness is set as the ending condition because the algorithm usually comes up to a satisfactory positioning result when the fitness drops down to 1×10^{-6}. In addition, the maximal iteration is set as the restarting condition. If the fitness failed to meet the ending condition after the maximal iteration, the positioning procedure will restart.

3.2 *Result and Analysis*

3.2.1 *Single-point test*

Figure 3 shows the convergence process of MAFSA when searching for the optimal 3-D coordinates to estimate the location of a test point. In Fig. 3, the red asterisk "*" is the test point whose 3-D coordinates is (1.5, 2.0, 1.0), whereas blue dots "·" represent the individuals of artificial fish in MAFSA. As shown in Fig. 3, all individuals of the artificial fish swarm are distributed randomly in the positioning space at first and then they move toward the best estimated point rapidly generation by generation. As can be seen in Fig. 3, when coming to the sixth generation, most individuals of the artificial fish are getting together in the neighborhood of the best estimated point. While finishing the 10th iteration, the whole swarm of artificial fish has gathered into a completely narrow region around the test point. Hitherto, the best state that has been reached is (1.4998, 1.9981, 0.9989) whose corresponding fitness is 2.202×10^{-6}.

Table 1 Parameters of the positioning simulation model.

Parameter	Value
Room size or search space (L × W × H)/m^3	4 × 4 × 6
Power of each LED bulb/W	10
Positions of each LED bulb (x, y, z)/m	LED 1 (0,4,6)
	LED 2 (4,4,6)
	LED 3 (4,0,6)
	LED 4 (0,0,6)
Height of the receiver/m	0.5 to 3.0 (resolution:0.5)
Plane range of the receiver/m	(0.25, 0.25) to (3.75, 3.75) (resolution:0.25)
The half-power angles of LED bulb/deg ($\phi_{1/2}$)	60
The FOV of receiver/deg (ψ_c)	90
The effective area of PD/cm^2	1.0
The photoelectric conversion efficiency/A · W^{-1} (r)	0.35
The gain of optical filter [$T_s(\psi)$]	1.0
The gain of optical concentrator [$G(\psi)$]	1.0
The population size of MAFSA	50
The ideal fitness of MAFSA	1×10^{-5}
The maximal iteration of MAFSA	20

Figure 4 shows the convergence tendency of the best fitness during the iteration process while Fig. 5 shows the variation trend of the 3-D positioning error. As can be seen, the tendencies of the two curves maintain a great consistency during the estimating process, which proves the correct establishment of the fitness function. In Fig. 4, the marked datum indicates that the 10th iteration is the first time when the best fitness declines to enough of a low level of 10^{-5} and meets the termination condition of the estimating procedure. Although the marked datum in Fig. 5 shows that the corresponding 3-D positioning error is ~2.2 mm, which is sufficient to be desirable. Judging from the analyses above, it is convincing that MAFSA is able to achieve a beautiful result within 20 or even less iterations in indoor 3-D positioning, which speaks volumes for the great real-time performance of the proposed system using MAFSA.

3.2.2 *Multipoint test*

As the single-point test mainly illustrates the positioning speed, the simulation on multiple point focusing on the positioning accuracy has also been done. Figure 6 shows the intuitionistic rendering of 3-D positioning tested at different heights of 0.5, 1.0, 1.5, 2.0, 2.5, and 3.0 m, at each of which, both the x and y coordinates of tested points vary from 0.25 to 3.75 m with a resolution of 0.25 m. Hence, there are 225 points tested in each plane and 1350 points involved totally in the positioning space. Judging from the rendering, in which red asterisks "*" represent the real points, whereas blue circles "o" represent the estimated points, it is distinct that there is not even a single point failing to be positioned with a macroscopic error. That proves the strong robustness of MAFSA.

To make a deeper assay of the positioning result of multipoint test, the statistic information is given below. In Fig. 7, the cumulative distribution function (CDF) curves of horizontal, vertical, and 3-D positioning errors are all presented, from which it is not difficult to discover that the vertical error plays a more important role in impacting the 3-D positioning error. As indicated by the curves in Fig. 7, if 90% is assumed as an acceptable service coverage rate, the proposed algorithm is able to deliver an accuracy of <5.95 mm in the 3-D room. That is to say, the proposed 3-D positioning system using MAFSA performs well in ensuring high positioning accuracy.

In Fig. 8, three histograms are given to show the statistical results about the numbers of 3-D positioning, horizontal, and

Downloaded From: https://www.spiedigitallibrary.org/journals/Optical-Engineering on 1/23/2019
Terms of Use: https://www.spiedigitallibrary.org/terms-of-use

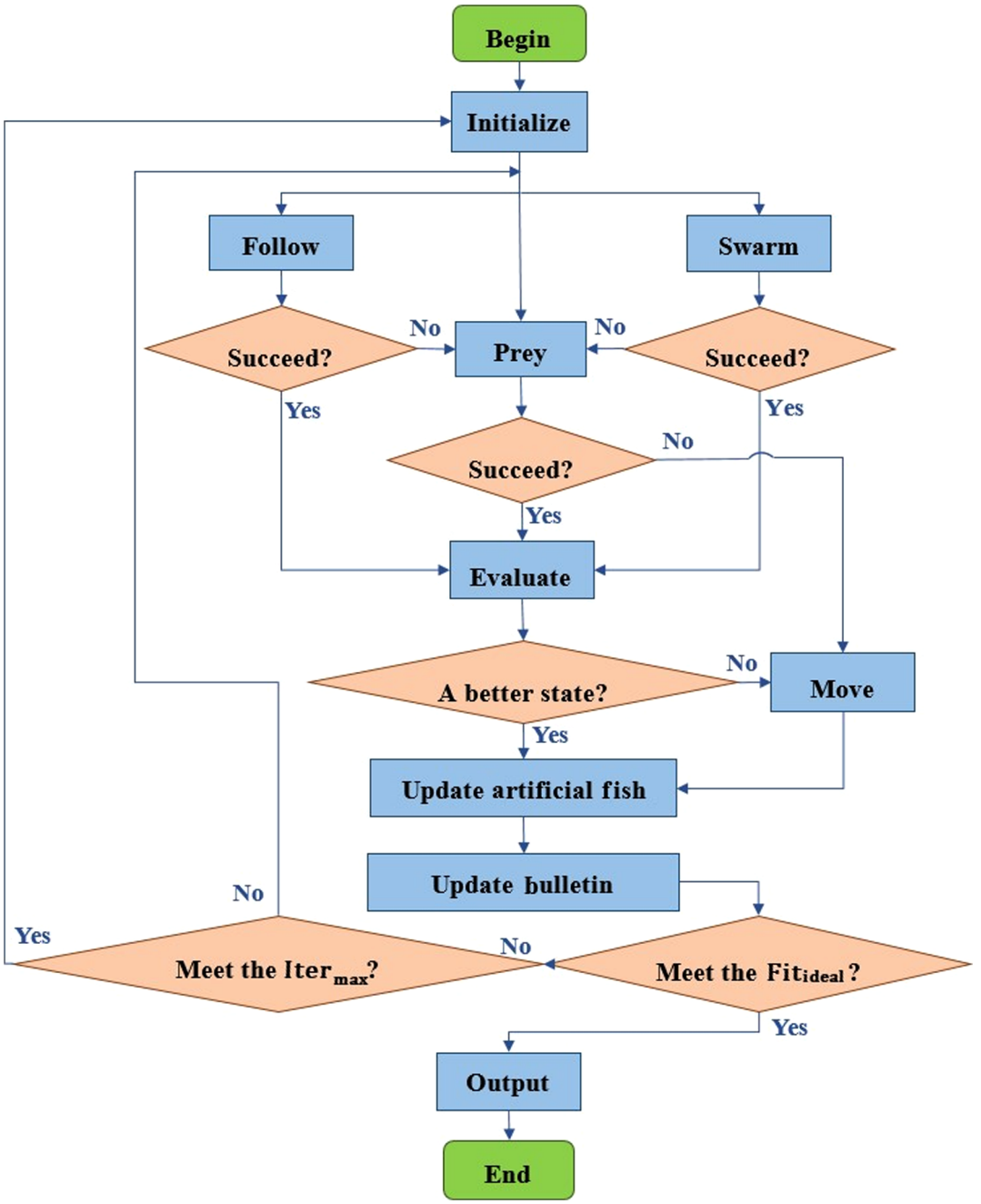

Fig. 2 The flow diagram of MAFSA.

vertical errors in different intervals. As most of the horizontal errors are below 4 mm while the vertical positioning errors vary from 0 to 2.33 cm, it can be educed that the vertical error is the dominant source of positioning error for the points with a 3-D positioning error over 1 cm. As is shown in Fig. 8(a), the 3-D positioning errors of most test points are within 7.5 mm. In addition, the maximum 3-D positioning error is 2.36 cm and the average 3-D positioning error is 4.05 mm, which further demonstrates the high accuracy of MAFSA comparing with other conventional algorithms. For example, in Ref. 28 the author proposed a Gaussian Process–Bayesian (CP-B) indoor localization method, which uses Gaussian Process to model the intensity distributions of the light sources and constructs a Bayesian localization framework using the results of the GP to precise localization. Though only 2-D positioning is taken into consideration, the mean error of the localization system is 0.56 m. While, as can be seen in Fig. 7, the maximum horizontal error of the proposed system using MAFSA is about 0.75 cm, which means that the MAFSA does much better than CP-B in positioning accuracy.

3.3 *Extended Simulation and Result Analysis*

3.3.1 *Positioning in motion scene*

In the simulation of positioning in a motion scene, the positioning target is assumed to move along the blue curve shown in Fig. 9 at a speed around 1 m/s. In view of the

Downloaded From: https://www.spiedigitallibrary.org/journals/Optical-Engineering on 1/23/2019
Terms of Use: https://www.spiedigitallibrary.org/terms-of-use

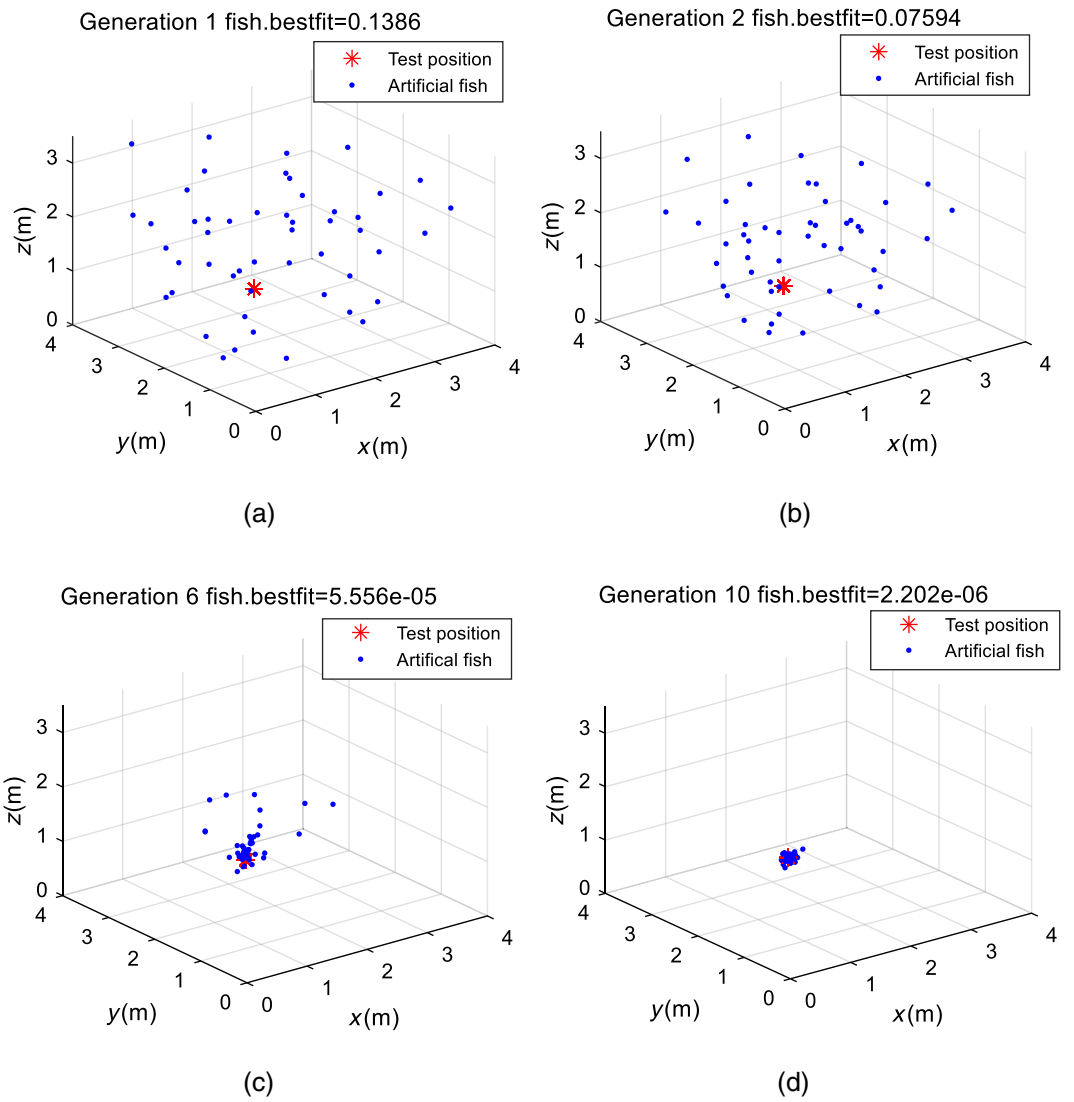

Fig. 3 (a)–(d) represent the distribution of the artificial fish swarm in the 1st, 2nd, 6th, and 10th generation, respectively.

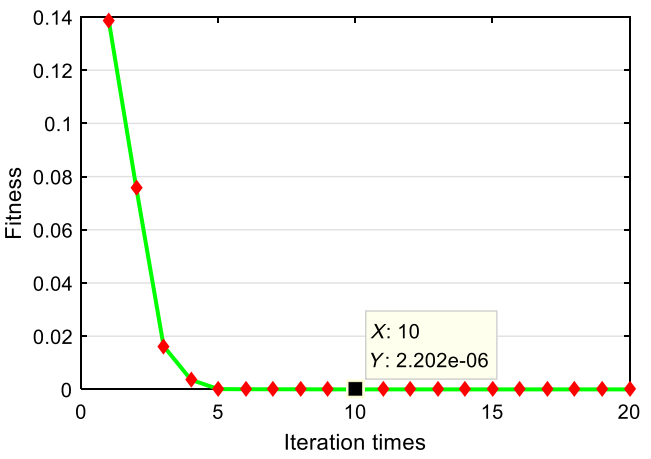

Fig. 4 The convergence graph of the best fitness.

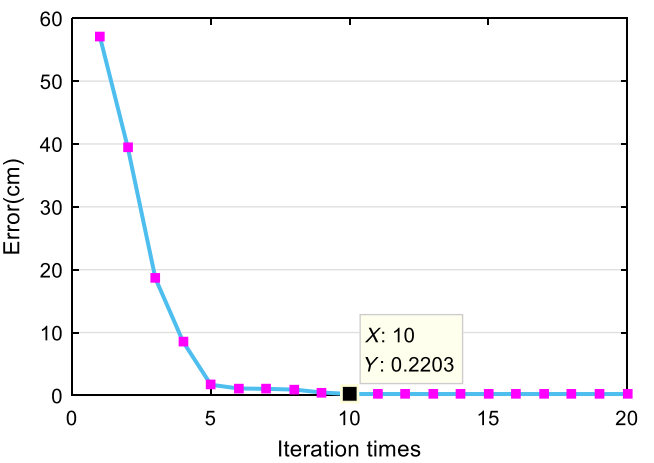

Fig. 5 The convergence graph of 3-D positioning error.

hysteresis of positioning, which mainly depends on the time the system requires to work out the position of terminal, an appropriate time interval should be set during the tracking process. To track the target, 76 points are sampled to be positioned with a time interval of 0.25 s, which is the average positioning time for each point measured in the simulation of multipoint test done in MATLAB 2016a on a computer (Lenovo XiaoXin 310-14ISK, Windows 10, 4G RAM,

Downloaded From: https://www.spiedigitallibrary.org/journals/Optical-Engineering on 1/23/2019
Terms of Use: https://www.spiedigitallibrary.org/terms-of-use

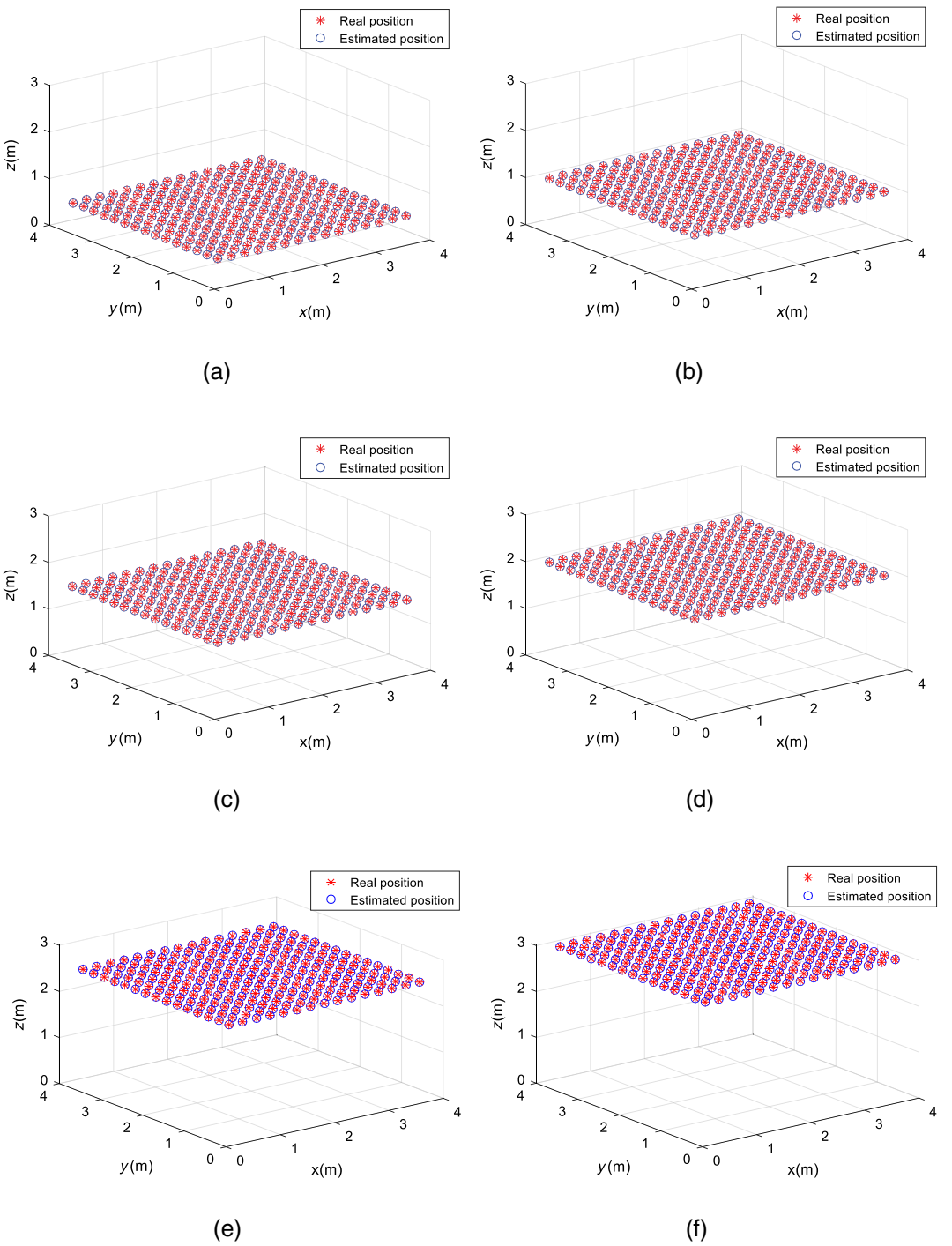

Fig. 6 The distribution of the real position and its estimated 3-D position: (a)–(f) represent the 3-D positioning results at the height of 0.5, 1.0, 1.5, 2.0, 2.5, and 3.0 m, respectively.

Intel Core i7-6500U @ 2.5 GHz). The estimated positions of the samples are shown in Fig. 9 by red crosses "×." Meanwhile, the horizontal view and vertical view of the whole tracking process are given in Fig. 10 in order that the tracking result can be observed more vividly. As shown in Figs. 9 and 10, all the estimated points fall precisely on the curve, which testifies that the positioning system is able to do a good job in the motion scene.

In Fig. 11, the CDF curves and histograms of the positioning errors indicate that the positioning errors of the sampled points are small enough to be satisfactory. If 94.74% is assumed as an acceptable service coverage rate, the proposed system is able to reach a high accuracy with a maximum 3-D positioning error of 5.48 mm. Moreover, even if all the samples are taken into consideration, the maximal 3-D positioning error is <7.25 mm and the average error is 3.57 mm, which proves the excellent performance of the proposed positioning system in the motion scene.

3.3.2 *Comparison between AFSA and MAFSA*

Different from all the foregoing simulations, the simulations in this section are carried out to compare the performances of

Downloaded From: https://www.spiedigitallibrary.org/journals/Optical-Engineering on 1/23/2019
Terms of Use: https://www.spiedigitallibrary.org/terms-of-use

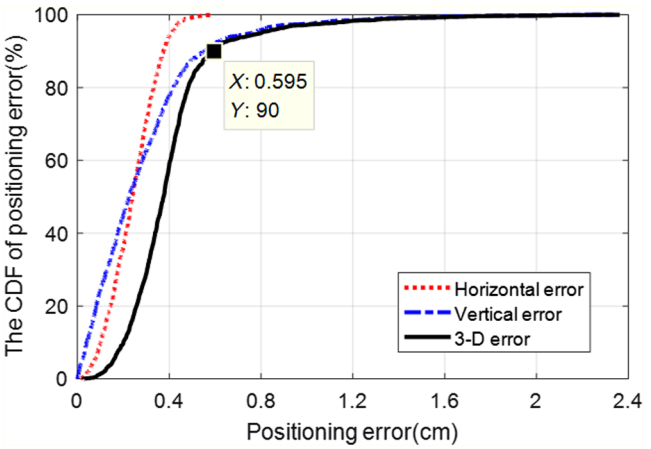

Fig. 7 The CDF curves of positioning errors.

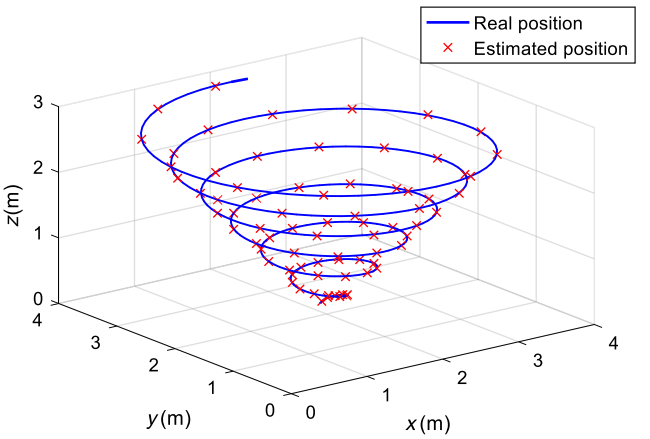

Fig. 9 The 3-D positioning result in motion scene.

AFSA and MAFSA so as to give evidence of the superiority of MAFSA. Continuously, the test point to be positioned is (1.5, 2.0, 1.0). In Fig. 12, the two curves show the convergence process of the new defined parameter Log10(Fitness), which represents Fitness and enlarges the imperceptible change of Fitness for clearer observation in the meantime. As Log10(Fitness) in MAFSA drops to -5.272 after the eighth iteration while in AFSA finally fails to meet the ending condition of -5 within 20 iterations, the convergence trend of Log10(Fitness) in MAFSA is much more rapid than in AFSA.

As for Fig. 13, it further demonstrates the rapidity of MAFSA comparing with AFSA by showing the CDF curves of iteration time. Here, the iteration time means the first time when the Fitness of an estimated point drops down to 10^{-5}, which is set as the termination condition of the iteration in both MAFSA and AFSA. As can be seen, if 92% of the test points are taken into consideration, the maximal iteration times of AFSA is 86, which is five times as much as that of MAFSA, approximately.

Judging from the simulation results of the comparison between the two algorithms, it is persuasive that MAFSA performs much better than the traditional AFSA, which

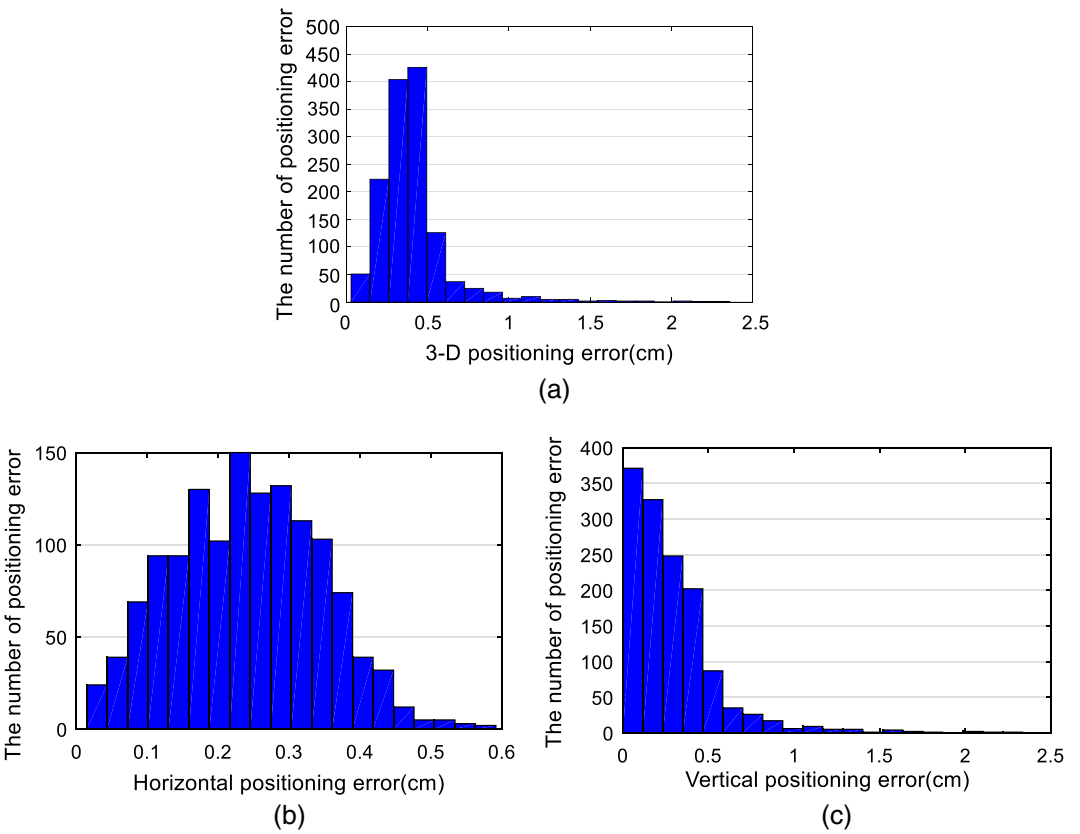

Fig. 8 The histogram of positioning errors. (a) 3-D positioning error (cm), (b) horizontal positioning error (cm), and (c) vertical positioning error (cm).

Downloaded From: https://www.spiedigitallibrary.org/journals/Optical-Engineering on 1/23/2019
Terms of Use: https://www.spiedigitallibrary.org/terms-of-use

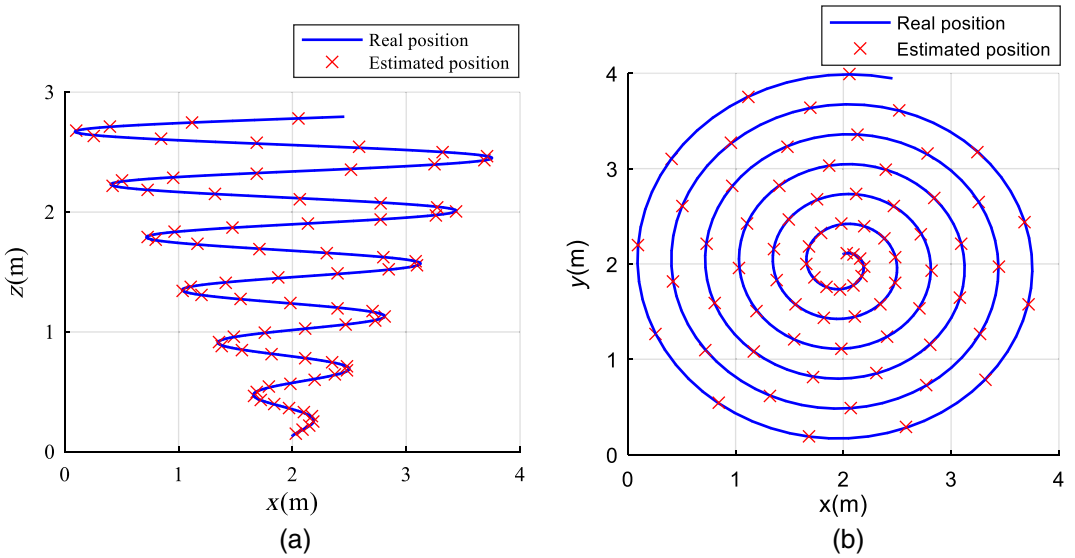

Fig. 10 (a) and (b) represent the principal view and vertical view of the 3-D positioning result in motion scene, respectively.

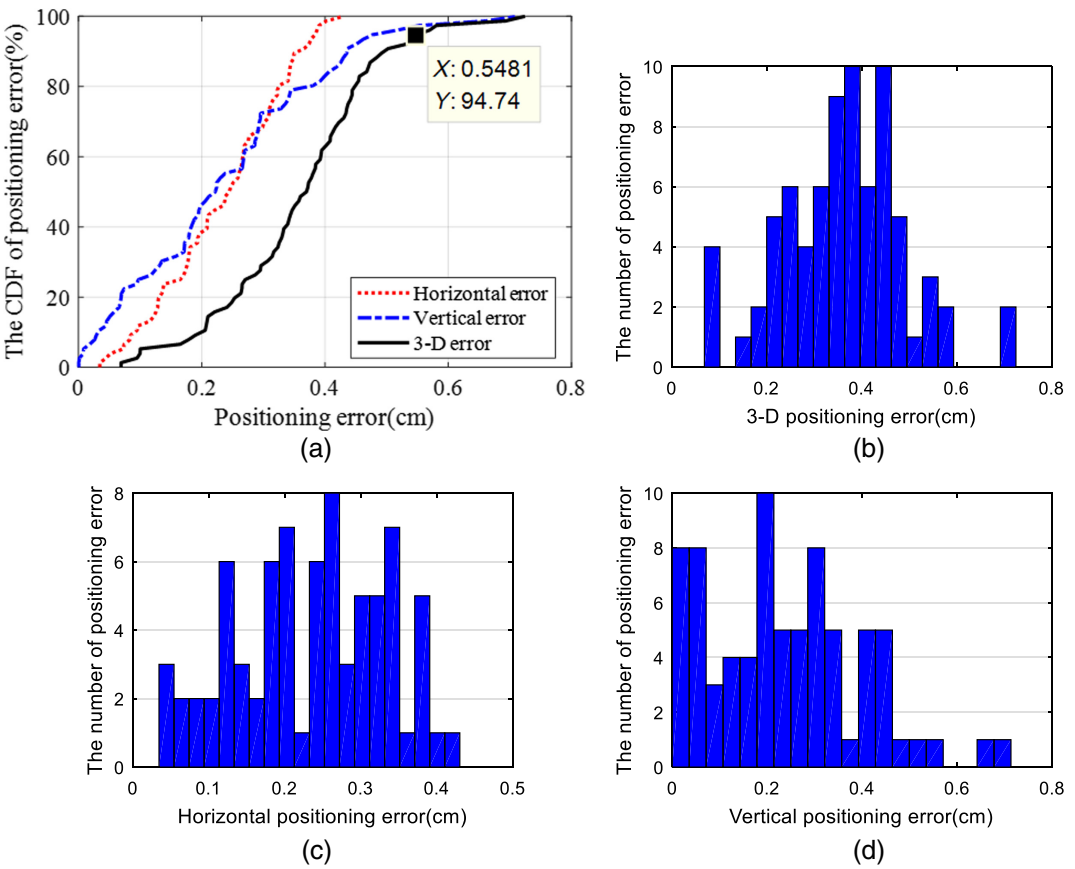

Fig. 11 The CDF curves and histogram of positioning errors in motion scene. (a) Positioning error (cm), (b) 3-D positioning error (cm), (c) horizontal positioning error (cm), and (d) vertical positioning error (cm).

confirms the significance of modifying the AFSA for indoor 3-D positioning based on VLC.

3.3.3 *Key parameter of MAFSA*

The number of artificial fish (NOAF) determines two important factors of MAFSA, including the search capability and the amount of calculation. On the one hand, the larger NOAF is, the stronger the search capability of the whole swarm is. On the other hand, an increase in NOAF leads to a greater amount of computation. Moreover, the search capability influences the required positioning time (RPT) of the system by affecting the convergence of MAFSA and the amount of

Downloaded From: https://www.spiedigitallibrary.org/journals/Optical-Engineering on 1/23/2019
Terms of Use: https://www.spiedigitallibrary.org/terms-of-use

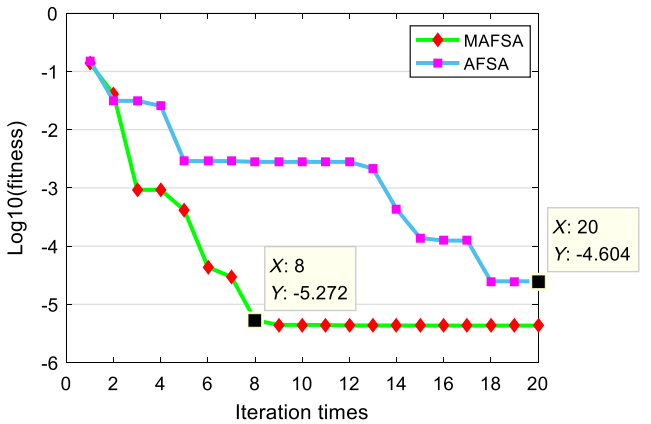

Fig. 12 The relationship between Log10(Fitness) and iteration time for the two algorithms.

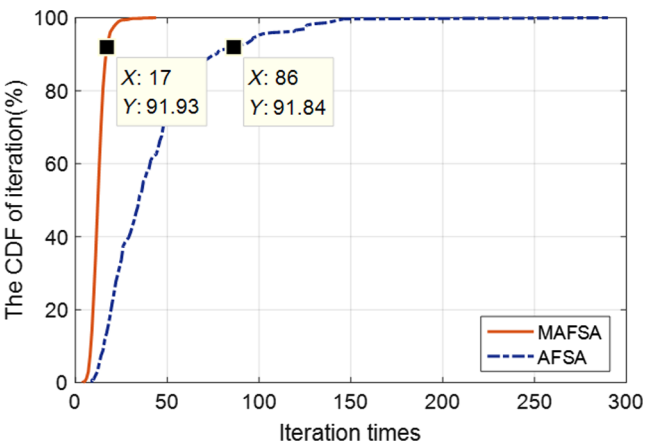

Fig. 13 The CDF of iteration time for the two algorithms.

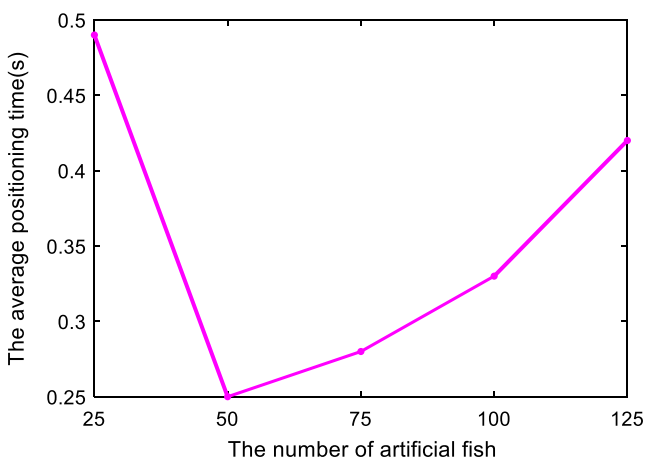

Fig. 14 The positioning time varies with the number of artificial fish.

calculation influences RPT of the system directly. In the other words, it is RPT of the system that NOAF eventually influences. Therefore, an extended simulation has been done in MATLAB2016a on the computer (Lenovo XiaoXin 310-14ISK, Windows 10, 4G RAM, Intel Core i7-6500U @ 2.5 GHz) to analyze the relationship between RPT and NOAF and the test points in this simulation are the same as those in the multipoint test. In Fig. 14, the line chart shows the corresponding relation between the average positioning time of the test points and the NOAF set in MAFSA. It is obvious that NOAF should not set too small or too big because both of the cases lead to a long positioning time and an appropriate value of NOAF in MAFSA for the proposed system is 50.

4 Conclusions

In this paper, a high-precision indoor 3-D positioning system based on VLC using MAFSA is proposed. As AFSA is a powerful population-based bionic evolutionary algorithm for global optimization problems, the positioning problem is transformed into a global optimization problem so as to be better solved using the mentioned algorithm. Moreover, to accelerate the convergence, AFSA is improved by ignoring the crowding factor of artificial fish swarm. To analyze the performance of the proposed system, a series of simulations are executed in a positioning space of 4 m × 4 m × 6 m. On one hand, the positioning accuracy is discussed in the simulations of multipoint test and target tracking test. Among them, the result of multipoint test shows that the average error of 3-D positioning is 4.05 mm and that 90% of positioning errors are below 5.95 mm. While in the target tracking test, >95% of the 3-D positioning errors are <5.74 mm and the average error is 3.67 mm. On the other hand, the positioning speed is discussed in the single-point test, which shows the rapid convergence of estimation. Furthermore, the superiority of the modified AFSA (MAFSA) is demonstrated by the simulations, which show that MAFSA has a higher convergence speed compared with AFSA. In conclusion, the results of simulations suggest that the proposed scheme is quite a promising solution to VLC-based indoor 3-D positioning on account of its excellent performance.

Acknowledgments

This work was supported by the National Undergraduate Innovative and Entrepreneurial Training Program (Nos. 201510561003, 201610561065, 201610561068, 201710561006, 201710561054, 201710561057, 201710561058, 201710561199, 201710561202, 201810561217, 201810561195, 201810561218, and 201810561219), Special Funds for the Cultivation of Guangdong College Students' Scientific and Technological Innovation ("Climbing Program" Special Funds) (pdjh2017b0040, pdjha0028), Guangdong Science and Technology Project (2017B010114001).

References

1. T. H. Do and M. Yoo, "An in-depth survey of visible light communication based positioning systems," *Sensors* **16**(5), 678 (2016).
2. H. Wang et al., "Study on improvement of fingerprint matching algorithm in wireless LAN based indoor positioning system," in *IEEE/ACIS Int. Conf. on Software Engineering, Artificial Intelligence, Networking and Parallel/Distributed Computing*, pp. 275–280, IEEE (2016).
3. R. Faragher and R. Harle, "Location fingerprinting with bluetooth low energy beacons," *IEEE J. Sel. Areas Commun.* **33**(11), 2418–2428 (2015).
4. C. H. Huang et al., "Real-time RFID indoor positioning system based on Kalman-filter drift removal and Heron-bilateration location estimation," *IEEE Trans. Instrum. Meas.* **64**(3), 728–739 (2015).
5. W. Vinicchayakul et al., "Study on performance of ultra wideband and narrow band propagation for an indoor positioning," in *IEEE Int. Colloquium on Signal Processing & its Applications*, pp. 194–198, IEEE (2016).

Downloaded From: https://www.spiedigitallibrary.org/journals/Optical-Engineering on 1/23/2019
Terms of Use: https://www.spiedigitallibrary.org/terms-of-use

6. D. Hauschildt and N. Kirchhof, "Advances in thermal infrared localization: challenges and solutions," in *Int. Conf. on Indoor Positioning and Indoor Navigation*, pp. 1–8, IEEE (2010).
7. H. Chen et al., "Indoor high precision three-dimensional positioning system based on visible light communication using modified genetic algorithm," *Opt. Commun.* **413**, 103–120 (2018).
8. W. Guan et al., "High-precision approach to localization scheme of visible light communication based on artificial neural networks and modified genetic algorithms," *Opt. Eng.* **56**(10), 106103 (2017).
9. W. Guan et al., "Performance analysis and enhancement for visible light communication using CMOS sensors," *Opt. Commun.* **410**, 531–551 (2018).
10. Y. Cai et al., "Indoor high precision three-dimensional positioning system based on visible light communication using particle swarm optimization," *IEEE Photonics J.* **9**(6), 1–20 (2017).
11. M. Dakkak et al., "Indoor localization method based on RTT and AOA using coordinates clustering," *Comput. Networks* **55**(8), 1794–1803 (2011).
12. A. Shi et al., "Impact of multipath effects on theoretical accuracy of TOA-based indoor VLC positioning system," *Photonics Res.* **3**(6), 296 (2015).
13. T. H. Do and M. Yoo, "TDOA-based indoor positioning using visible light," *Photonic Network Commun.* **27**(2), 80–88 (2014).
14. S. H. Yang, E. M. Jung, and S. K. Han, "Indoor location estimation based on LED visible light Communication using multiple optical receivers," *IEEE Commun. Lett.* **17**(9), 1834–1837 (2013).
15. S. H. Jung et al., "Received signal strength ratio based optical wireless indoor localization using light emitting diodes for illumination," in *IEEE Int. Conf. on Consumer Electronics*, pp. 63–64, IEEE (2013).
16. B. N. Vellambi, M. Yasir, and S. W. Ho, "Indoor positioning system using visible light and accelerometer," *J. Lightwave Technol.* **32**(19), 3306–3316 (2014).
17. Y. Hou et al., "A RSS/AOA based indoor positioning system with a single LED lamp," in *Int. Conf. on Wireless Communications & Signal Processing*, pp. 1–4, IEEE (2015).
18. J. Lim, "Ubiquitous 3D positioning systems by led-based visible light communications," *Wirel. Commun. IEEE* **22**(2), 80–85 (2015).
19. J. Li, L. Zhang, and H. Ma, "A new positioning method combining GA and iterative LS algorithm in NLOS environment," in *IEEE 9th Int. Conf. on Communication Software and Networks (ICCSN)*, Guangzhou, pp. 403–407 (2017).
20. L. C. Lai et al., "Position estimation of a mobile robot by PSO algorithm using a laser range finder," in *Int. Conf. on Consumer Electronics, Communications and Networks*, pp. 1505–1508, IEEE (2011).
21. L. I. Xiaolei, Z. Shao, and J. Qian, "An optimizing method based on autonomous animals: fish-swarm algorithm," *Syst. Eng.-Theory Pract.* **22**(11), 32–38 (2002).
22. Y. Baba, O. C. Ugweje, and G. Koyunlu, "Development and analysis of a modified artificial fish swarm algorithm," in *Electronics, Computer and Computation (ICECCO)*, pp. 1–6 (2017).
23. W. Guan et al., "Errata: high precision three-dimensional iterative indoor localization algorithm using code division multiple access modulation based on visible light communication," *Opt. Eng.* **55**(10), 106105 (2016).
24. W. Guan et al., "Indoor positioning technology of visible light communication based on CDMA modulation," *Acta Opt. Sin.* **36**(11), 73–81 (2016).
25. W. Guan et al., "A novel three-dimensional indoor positioning algorithm design based on visible light communication," *Opt. Commun.* **392**, 282–293 (2017).
26. Y. Hou et al., "Single LED beacon-based 3-D indoor positioning using off-the-shelf devices," *IEEE Photonics J.* **8**(6), 1–11 (2016).
27. T. Komine and M. Nakagawa, "Fundamental analysis for visible-light communication system using LED lights," *IEEE Trans. Consum. Electron.* **50**(1), 100–107 (2004).
28. K. Qiu, F. Zhang, and M. Liu, "Visible light communication-based indoor localization using Gaussian process," in *IEEE/RSJ Int. Conf. on Intelligent Robots and Systems*, pp. 3125–3130, IEEE (2015).

Shangsheng Wen received his BE degree from Wuhan University of Science and Technology in 1984, his ME degree from Anhui Institute of Optics and Fine Mechanics, Chinese Academy of Sciences in 1993, and his PhD from South China Normal University in 2001. He is a professor at the State Key Laboratory of Luminescent Materials and Devices. He has undertaken more than 20 scientific research projects and published hundreds of papers. His research focus on visible light communication.

Xiaoge Cai is now studying at South China University of Technology in the automation science and engineering department for her BE degree. Her research interests currently concentrate on the area of visible light wireless communication technology and indoor positioning technology.

Weipeng Guan obtained his BE degree from the electronic science and technology department (electronic materials and components department) in South China University of Technology, Guangzhou, China, in 2016. He is now working toward his ME degree in the control theory and control engineering department at South China University of Technology. His research is focused on visible light wireless communication technology and visible light positioning technology.

Jiajia Jiang is now studying at South China University of Technology in the information engineering department for her BE degree. Her research is currently focused on visible light wireless communication technology.

Bangdong Chen is currently studying at South China University of Technology at information engineering department for his BE degree. His research interests are in wireless optical communication technology and visible light positioning technology.

Mouxiao Huang is now studying at South China University of Technology in the automation science and engineering department for his BE degree. His research is focused on visible light wireless communication technology and indoor positioning technology.

Downloaded From: https://www.spiedigitallibrary.org/journals/Optical-Engineering on 1/23/2019
Terms of Use: https://www.spiedigitallibrary.org/terms-of-use